Agilent

Trusted Answers

Fast, Automated Microplastics Analysis Using Laser Direct Chemical Imaging

Characterizing and quantifying microplastics in water samples from marine environments

Authors

Lars Hildebrandt, Fadi El Gareb, Tristan Zimmermann, Ole Klein, Kay-Christian Emeis, Daniel Proefrock[1] Andreas Kerstan[2]

[1]Institute of Coastal Research, Helmholtz-Zentrum Geesthacht, Germany
[2]Agilent Technologies

Introduction

It is estimated that more than 75% of the 8.3 billion metric tons of plastic produced over the last 65 years have turned into waste (*1*). Up to 13 million metric tons of this waste ends up in the ocean every year (*2*) and recent calculations estimate that more than 5.25 trillion plastic particles float in the world's oceans (*3*).

Scientists have demonstrated the alarming environmental ubiquity and persistence of particulate plastic in aquatic ecosystems (*4*). Models predict that approximately 14% of the plastic debris in the ocean surface layer can be classified as so-called microplastics (often referred to as particles between 1 µm and 5 mm in size) (*5*). These ingestible and potentially harmful particles have been formed by UV-induced, mechanical, or biological degradation of larger debris items (*6*). To verify the estimates and to meet upcoming regulatory measures (e.g., California Senate Bill 1422) and directives (MSFD, 2008/56/EC), accurate, time-efficient, and robust analytical workflows and techniques are required.

Suitable techniques should determine the size, shape and polymer type of microplastic particles and provide fast quantification of each type. At the time of writing, a lack of harmonization and standard operation procedures (SOPs) has led many studies to rely on either visual identification, or manual Fourier Transform Infrared (FTIR) or Raman-based analysis of suspected particles. These techniques are very time-consuming and may be prone to operator bias. In this work, we present an innovative microplastics analysis workflow using laser direct infrared imaging.

Experimental

The lack of standard operating procedures for microplastics sample preparation and analysis has resulted in many applied methods that are prone to contamination, not time-efficient, or that only enable processing of non-representative low water volumes (7). Procedures covering all stages of the analytical chain were developed and applied in this study, including sampling, matrix digestion and micro-spectroscopic analysis utilizing LDIR. Extensive contamination prevention measures and deposition controls were undertaken. Procedural blanks were utilized to quantify remaining contamination. All laboratory work was carried out on clean benches (laminar flow cabinets) both in the lab and on board the research vessel. The benches had approximately 99.995% air filtration efficiency for particles larger than 0.1 microns (according to the EN1822 1 standard). Additionally, Dustbox air purifiers[1] were run in all laboratories to filter the air.

Sampling

Samples were collected in the Indian Ocean during the Sonne 270 (2019) cruise from Hong Kong to Port Louis (Figure 1). The area sampled covered a large area of ocean, spanning from a region to the west of Indonesian Sumatra through to an area to the east of Madagascar.

Figure 1. The sampling location stations along the transect in the Indian Ocean.

Sampling was conducted utilizing the Geesthacht Inert Microplastic Fractionator (GIMPF), as shown in Figure 2, to filter high volumes of suspended particulate matter (SPM, 10 μm ≤ d_{SPM}) from ocean water. The dual-channel GIMPF enabled online SPM fractionation (by two different mesh sizes of stainless steel cartridge filters) into the size classes > 300 μm and 10 μm ≤ d ≤ 300 μm. The flow-through system was fed with seawater from the ship′s moon pool at 6 m below sea level. The entire sampling system was constructed of stainless-steel parts (AISI-316L) and mounted on an aluminum plate. All seals were PFA-sheathed to minimize risk of contamination by the sampling system. After every sampling location, the system was backflushed over a 2 μm filter on the backside of the GIMPF. Up to 61 m³ was sampled in total. From the cartridge filters, the samples were vacuum-filtered onto PTFE and PC membranes (5 μm pore size) and stored in amber glass bottles.
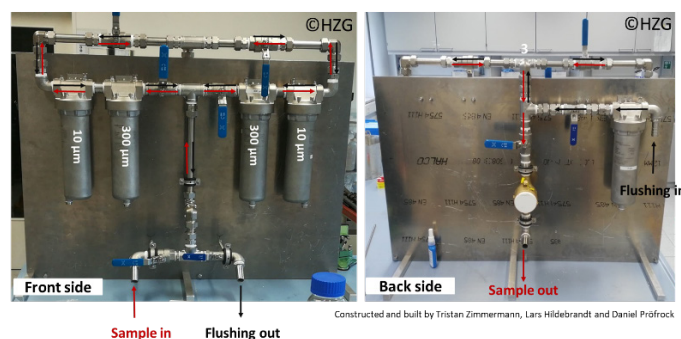

Figure 2. Front and back of the Geesthacht Inert Microplastic Fractionator (GIMPF).

Sample preparation and method validation

All glassware was rinsed three times with Milli Q water and pre-filtered ethanol (30%) before usage. In order to remove interfering natural organic and inorganic matrix constituents, the size fraction with 10 μm ≤ d ≤ 300 μm was subjected to an enzymatic and oxidative digestion protocol. Briefly summarized, the samples were treated with Proteinase K, H_2O_2 in conjunction with Fe^{2+} catalyst and chitinase (Figure 3) followed by density separation using $ZnCl_2$ solution (ρ = 1.7 g mL^{-1}).
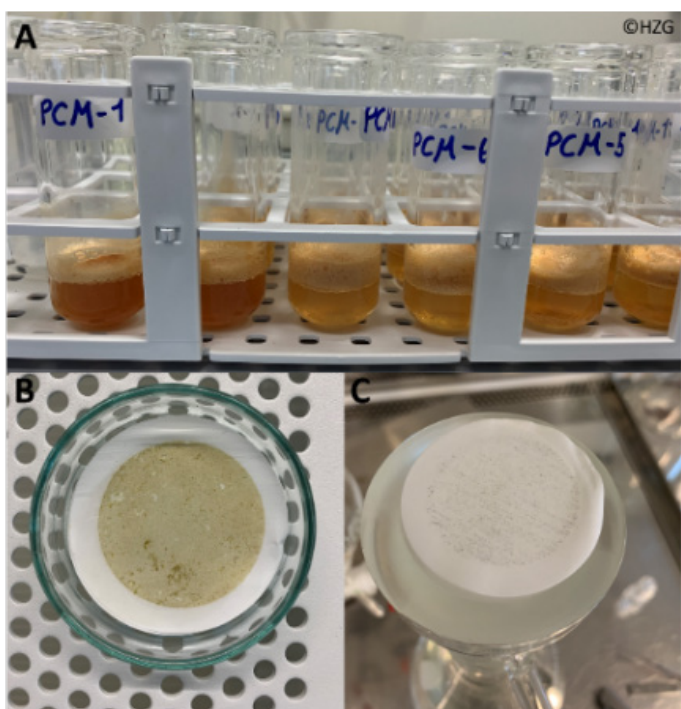
Figure 3. Enzymatic and oxidative digestion. **A**: Catalytic decomposition of remaining H_2O_2 by Fe^{2+}. **B**: Sample before matrix digestion (on a PTFE membrane). **C**: Sample after matrix digestion.

Instrumentation

To identify and quantify microplastics in the samples, an Agilent 8700 LDIR Chemical Imaging System was used. The LDIR, a name derived from its mode of operation, laser direct infrared imaging, utilizes a Quantum Cascade Laser (QCL) as the source. The QCL is a semi-conductor-based laser in which electrons tunnel through a series of quantum wells and emit light, allowing it to be rapidly tuned through the wavenumber (λ^{-1}) range, in this case 1800 cm^{-1} to 975 cm^{-1}. When combined with a single-point mercury cadmium telluride (MCT) detector (thermometrically cooled) and rapid scanning optics, two useful modes of action arise. In the first, the LDIR selects a single wavelength and scans through the objective as it moves over the sample at a very high speed. In the second mode, the objective is parked at a single point, while the QCL sweeps through the range, obtaining a full spectrum in less than one second.

The microplastics analysis workflow utilized both modes. The scanning mode was first used to rapidly scan the sample area at a single wavenumber. The resulting IR image was used to both locate particles in the sample and describe their size and shape. Once located, the LDIR then rapidly and automatically moved to each particle and acquired a full spectrum in the covered range. Once a spectrum was

acquired from a particle, it was immediately, and in real-time, compared to a microplastics spectral library. The best fit match for the spectrum was determined and reported for each particle. The library was derived from well-established sources and included a range of spectra relevant to the analysis of microplastics in marine water derived samples.

The instrument utilized a large field of view camera to obtain an entire view of the sample and a microscope-grade objective to capture high magnification visual images as needed. Fully automated analysis of 800 particles and comparison of the generated spectra to the database took about 1 hour to complete.

Sample analysis

Purified samples (< 300 µm) were suspended in ethanol (50%) and deposited on infrared reflective glass slides (7.5 × 2.5 cm; MirrIR, Kevley Technologies). The glass slides were analyzed in transflection by automated LDIR (QCL) Imaging (8700 LDIR, Agilent Technologies). The automated particle analysis protocol within the Agilent Clarity software (version 1.1.2) that operates the LIDR was used for all analysis. Sensitivity was set to the maximum and the spectral resolution to 8 cm^{-1}. Particles in the size range 20 - 5000 µm were analyzed, but can be extended down to approximately 10 µm in the automated mode.

The automated workflow within the Agilent Clarity software acquires IR spectra from each particle and, in real-time, conducts the spectral database comparison (> 420 reference spectra) and data processing. The statistics as well as the thresholds for a positive assignment were adapted according to the analysis. After running the automated workflow, the results were manually checked in transflection mode and partially by means of the LDIR's µ-ATR function.

Potential microplastics particles and fibers with d >300 µm were analyzed by ATR-FTIR spectroscopy (on a diamond or germanium crystal) and also by the LDIR using both transflection mode and its µ-ATR unit. The ATR-FTIR spectra were compared to the siMPle database (https://simple-plastics.eu). However, the fraction >300 µm will not be discussed in detail in this note.

Method validation

As yet, there are no certified reference materials of microplastics available on the market. Thus, validation was conducted by means of in-house reference PE, PET, PP and PVDC particles (20 - 500 µm) (7). More than 95% of the particles were correctly identified using the workflow described above. A matrix-matched certified reference material (Plankton, BCR-414, JRC) was also analyzed (Figure 4). Both analyses were used to extend the spectral library of the LDIR 8700, with IR spectra of natural and anthropogenic particles being added.
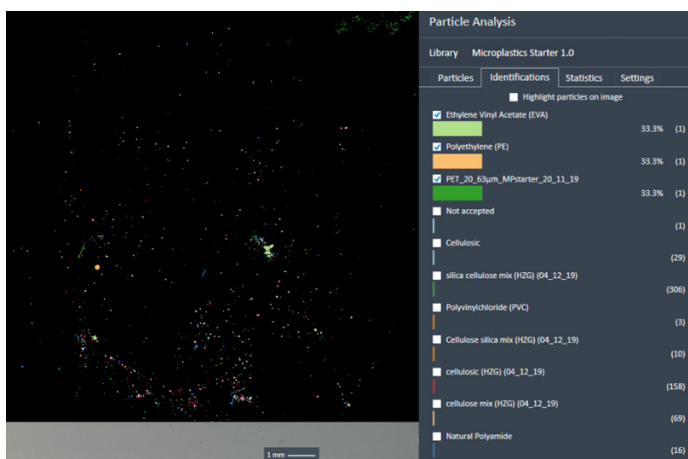
Figure 4. False-color IR image and polymer type statistics of reference certified reference plankton material (BCR-414) derived from automated LDIR analysis workflow.
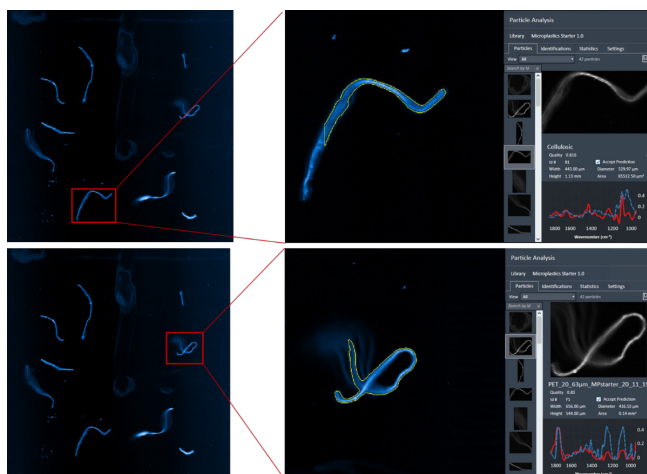

Figure 6. These fibers, > 300 μm, were identified to be cellulosic (upper image; containing indigo dye confirmed by Raman analysis), PET (lower image) and PP (not shown). There was 100% agreement between ATR-FTIR spectroscopy and LDIR Imaging for these fibers.

Results and discussion

Microplastic concentrations (>20 μm) for the sampling locations 1 - 7 ranged from 10 to 226 particles/fibers m^{-3} (Table 1). 30,471 natural, 635 synthetic particles and 14 different polymer clusters were identified in the 7 samples. The most abundant polymer clusters were acrylates/polyurethanes/varnish (39.2%) PET (26.0%), PE-Cl (7.1%), PVC (6.0%), PE (5.2%), PP (5.2%) and rubber (4.3%). 94.9% of the microplastics particles/fibers had a diameter <100 μm (Figure 5).
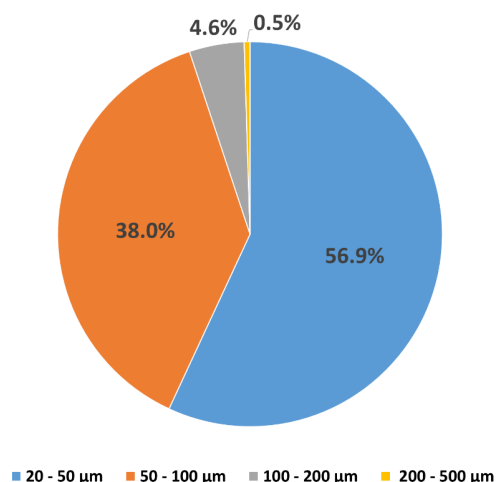
Even after almost complete matrix removal, 97.4% of the identified particles had a natural origin (cellulosic, silicate, coal, chitin and natural polyamide IR spectra), whereas only 2.6% were assigned to synthetic polymer types (Figure 7). Domogalla-Urbansky *et al*. (2018) describe microplastics particle / natural particles ratios between 1:100 and 1:1000 (also after sample preparation) (*8*).

Figure 5. Percentages of the different size classes of the identified microplastic particles/fibers.
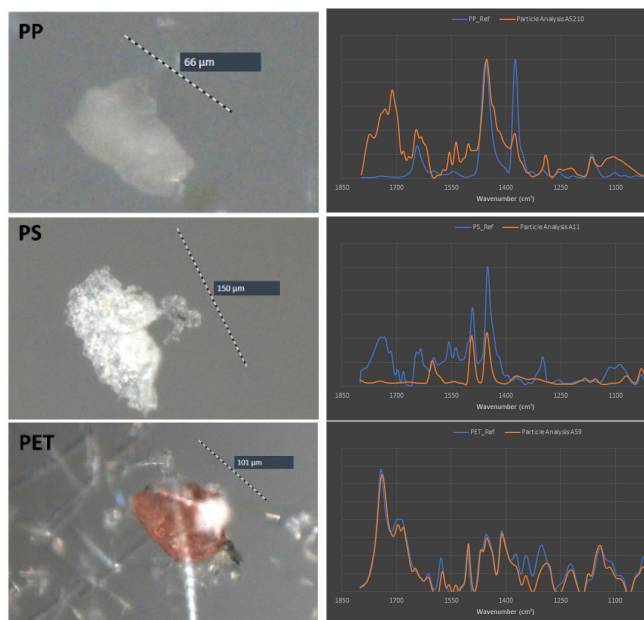

Figure 7. Different types of microplastics detected in water samples (<300 μm) from the Indian Ocean. The polypropylene (top) and polystyrene (middle) spectra were manually recorded, whereas the polyethylene terephthalate (bottom) spectrum was from the automated analysis.

Table 1. The filtered volume, sample location and the number of microplastics detected for each station. The most abundant polymer types for each is also listed.

Station	Sampled Volume [m³]	Coordinates	Number of Particles/Fibers	Number of Microplastics Particles/Fibers	Most Abundant Microplastics Type (#)	Microplastics Concentration [MPs m-3]
1	2.3	07°17.86'S, 97°45.85'E	3150	47	PET (20)	21
2	5.7	07°33.607'S 95°59.252'E	524	54	PET (32)	10
3	1.1	08°08.165'S 92°05.016'E	2112	67	PP (22)	62
4	1.3	08°20.93'S 90°38.76'E	16687	293	Acrylates/ Polyurethanes/ varnish (116)	226
5	1.3	08°55.25'S 86°45.32'E	2938	109	PET (40)	86
6	1.4	09°06.639'S 85°27.92'E	5110	239	Acrylates/ Polyurethanes/ varnish (69)	165
7	1.4	09°32.11'S 82°34.58'E	857	15	PS (5)	11

In contrast to other studies, where only a percentage of the sample suspension or a small area of filtered sample was analyzed (9, 10), the digestion protocol and LDIR imaging of a large microscope slide enabled analysis of each entire sample. This measurement technique reduced the uncertainty introduced by any extrapolation.

As Figure 8 shows, it is important to use spectroscopic particle analysis and not just visual identification, as natural and colorless synthetic particles often have a similar appearance (even for beads).
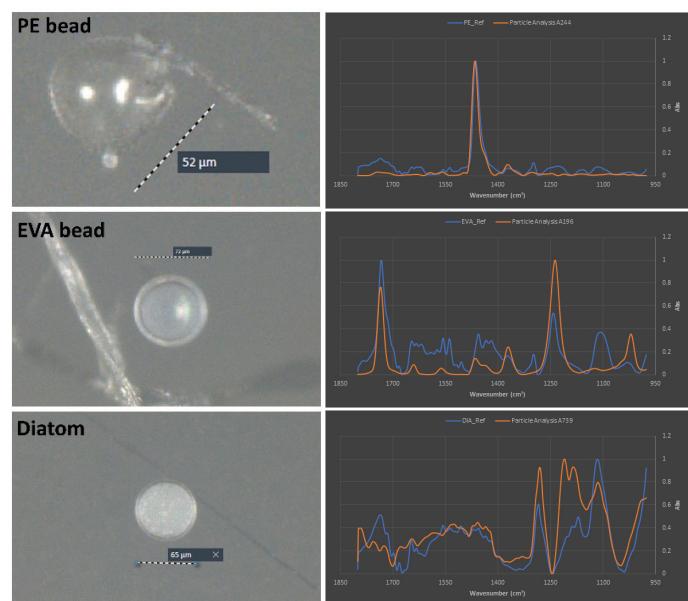

Figure 8. Visual images (left) and IR spectra (compared to the best-fit library spectrum) of two microplastic beads (PE and EVA). The lower image shows a diatom identified by LDIR analysis in the samples.

Figure 9 shows an example of how microplastic particles can be attached to natural particles e.g. diatoms. In this case, the LDIR's µ-ATR function was used to verify the polymer type (very good agreement with library spectrum). It was even possible to position the crystal directly on the particle attached to the diatom to cross check the result of the automated analysis.
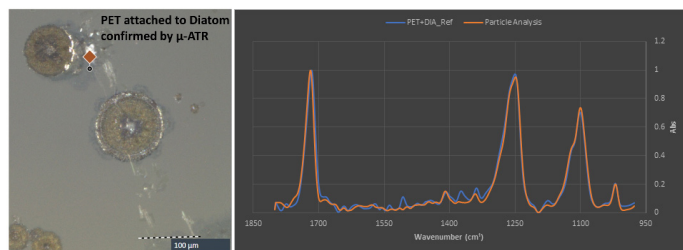

Figure 9. Visual images (left) and µ-ATR-IR spectrum (compared to the best-fit library spectrum) of a PET particle (indicated by the orange marker), attached to a diatom.

Based on a elongation factor (aspect ratio) of 3 (11), the majority of the microplastics were identified as fragments and not microfibers. Fiber recognition is quite challenging—especially for single-point imaging-based approaches, but LDIR Imaging can easily identify fibers (as shown in Figure 6) in environmental samples.

There is scientific consensus on the problem of measurement contamination due to airborne fibers (12). Consequently, the strict use of clean benches might explain the lower share of microfibers compared to other studies.
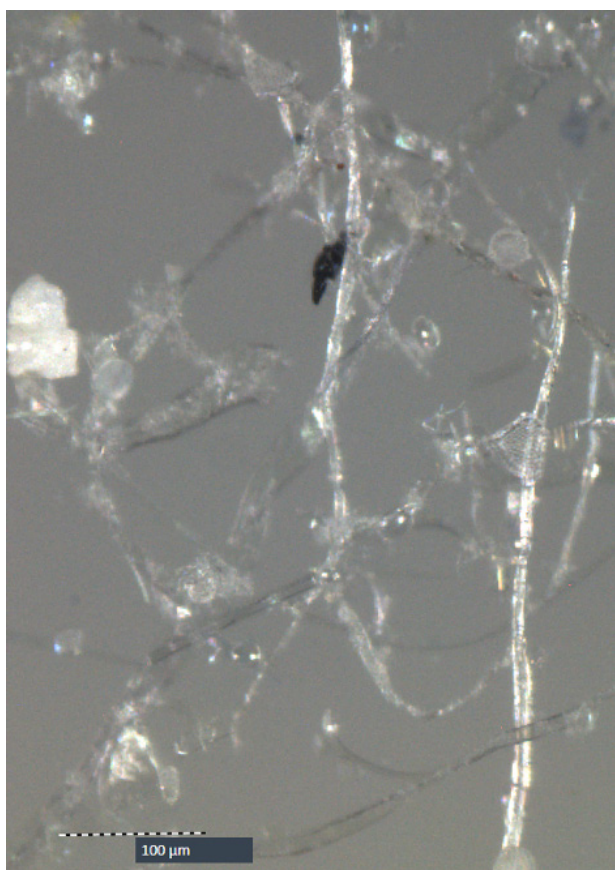
Figure 10. Visual image of an aggregate of the cellulose fibers and natural particles recorded by the LDIR.

To analyze entangled fibers (for included polymers) as well as particle aggregates (Figure 10), the manual single-peak (Figure 11) or hyperspectral imaging functions of the LDIR were applied.
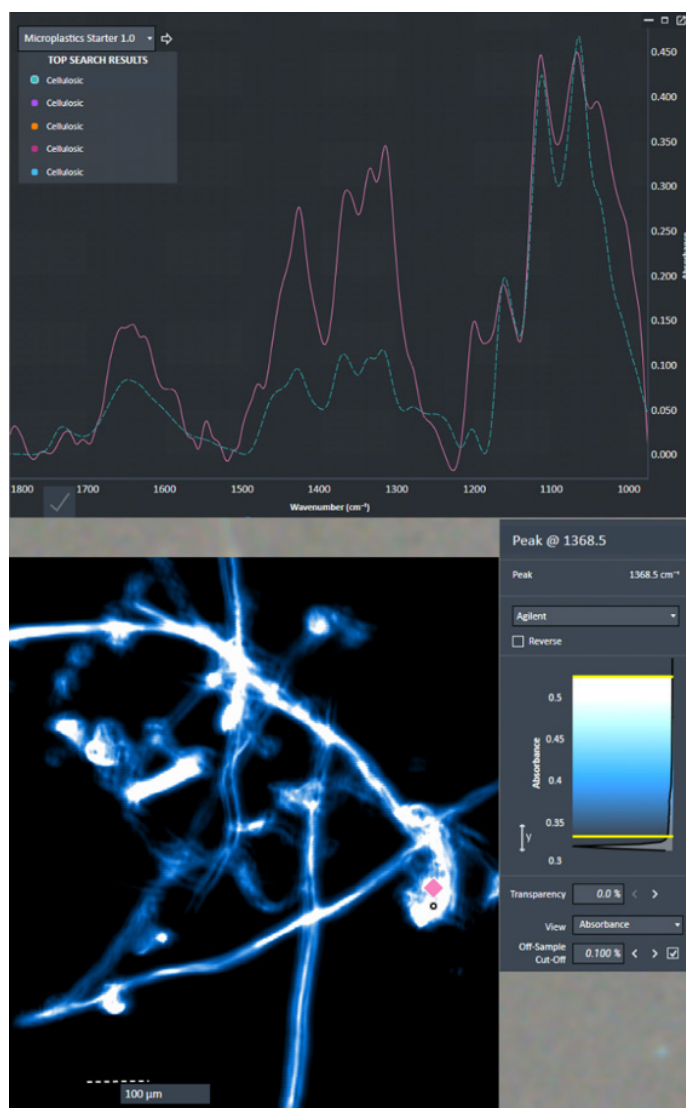

Figure 11. The IR single peak image at $\tilde{v}$ = 1368.5 cm^{-1} (lower, right) and IR spectrum (upper) of the aggregate of the cellulose fibers and natural particles shown in Figure 10.

Multi-peak analysis, in conjunction with the µ-ATR, proved valuable for particles containing biofilm-populated areas. Figure 12, for instance, shows a large polyurethane (PU) particle that exhibits areas showing clear cellulosic IR spectra and good PU and acrylate spectra. Both were confirmed by manual transflection and µ-ATR analysis. The LDIR enables good spatial differentiation between such different domains of environmental aggregates, but is also useful with respect to particles consisting of polymer blends and composites. Multi-peak can help to identify the different components of such mixtures in environmental microplastics.
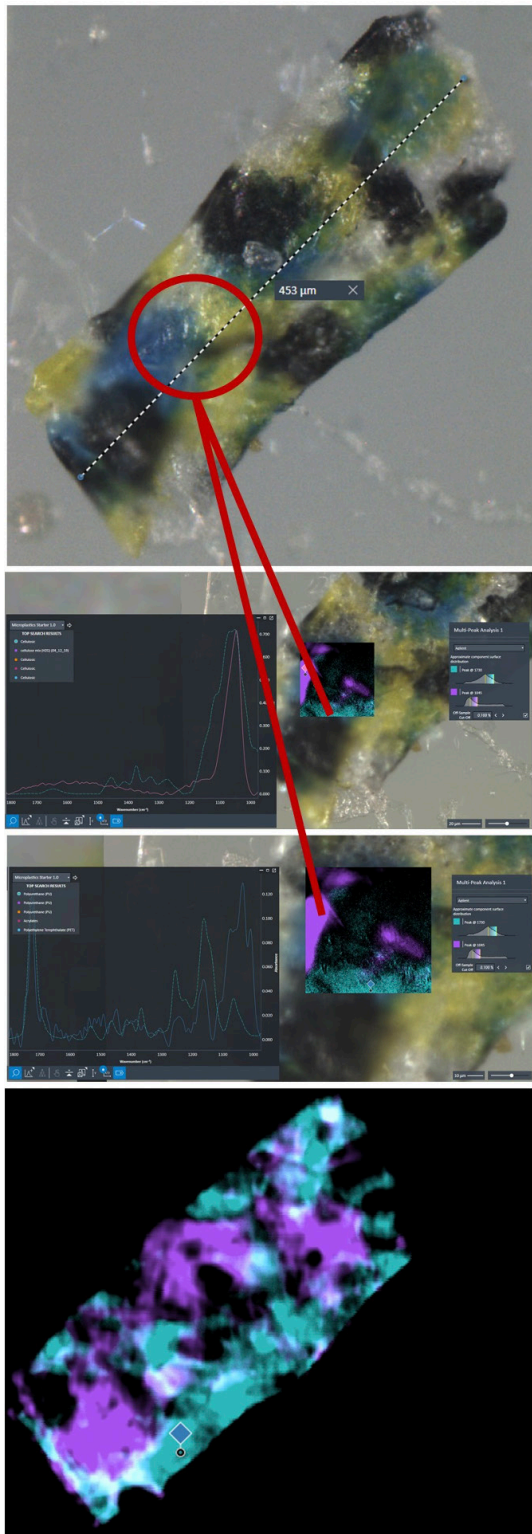
Figure 12. Presumably biofilm-populated PU particle (top) analyzed by multi-peak imaging (bottom) showing strong absorption at $\tilde{v}$ = 1045 cm^{-1} and $\tilde{v}$ = 1730 cm^{-1} (middle). Violet domains show good agreement with cellulosic reference spectra (2nd picture), whereas turquoise domains correspond to PU and Acrylate spectra (3rd picture).

Comparison to other microplastic studies

Even though inter-study comparison is hampered by the application of different methods (sampling and detection), the reported concentrations (10 - 226 MPs m^{-3}) are well in line with other studies based on either FTIR or Raman micro-spectroscopy. Lorenz *et al.* (2019) found between 0.1 and 245.4 microplastics particles m^{-3} in manta net samples from the southern North Sea (surface water) (9). Enders at al. (2015) detected between 13 and 501 MPs m^{-3} in samples taken with a fractionated filtration device in the Atlantic Ocean (3 m below water line) (*13*). According to modeling and monitoring data, microplastics concentrations in surface water can be up to 30-times higher compared to the water column (*14-16*). Therefore, it is likely that the sampled area exhibits a comparably high particulate plastic contamination, with high concentrations at the sea surface.

Polymer types detected in the study do seem to support this hypothesis. The 2nd (PET), 3rd (PE-Cl) and 4th (PVC) most abundant polymers found in this study have typical densities exceeding the density of seawater (first most abundant acrylates/polyurethanes/varnish can have a larger density spread). It is remarkable that the lower density polymers PE and PP (~ 50% production volume) both make up only 5.2% each of the found microplastics. These polymers remain at the surface until biofouling leads to sinking and transport to the seafloor. However, this hypothesis must be proven in the future by sampling at different depths (depth profiling).

Conclusion

LDIR imaging was successfully used to detect and characterize microplastic particles and fibers in high-volume marine water samples. Results indicated comparably high microplastic contamination.

The results of the automated workflow were thoroughly rechecked by visual inspection, at least 5 manual transflection IR measurements, and partially by μ-ATR IR analysis. For the fraction >300 μm, good agreement was achieved between LDIR imaging, using a well-established microplastics spectral database, and conventional ATR-FTIR analysis. Extension of the database with typical matrix spectra helped to further increase the accuracy of the workflow.

Due to its time-efficiency and high degree of automation, the technique has a great potential to become the micro-spectroscopic method of choice, e.g. during large scale microplastics studies or for monitoring activities, which require fast data provision.

References

1. Geyer, R., J.R. Jambeck, and K.L. Law, *Production, use, and fate of all plastics ever made*. Science Advances, **2017**, 3(7): p. e1700782.

2. Jambeck, J.R., R. Geyer, C. Wilcox, T.R. Siegler, M. Perryman, A. Andrady, R. Narayan, and K.L. Law, *Plastic waste inputs from land into the ocean*. Science, **2015**, 347(6223): p. 768.

3. Eriksen, M., L. Lebreton, H. Carson, M. Thiel, C. Moore, J. Borerro, F. Galgani, P. Ryan, and J. Reisser, *Plastic Pollution in the World's Oceans: More than 5 Trillion Plastic Pieces Weighing over 250,000 Tons Afloat at Sea*. PLoS ONE, **2014**, 9.

4. Ivleva, N.P., A.C. Wiesheu, and R. Niessner, *Microplastic in Aquatic Ecosystems*. Angewandte Chemie International Edition, **2017**, 56(7): p. 1720-1739.

5. Koelmans, A., M. Kooi, K. Law, and E. Sebille, *All is not lost: Deriving a top-down mass budget of plastic at sea*. Environmental Research Letters, **2017**, 12.

6. Song, Y.K., S.H. Hong, M. Jang, G.M. Han, S.W. Jung, and W.J. Shim, *Combined Effects of UV Exposure Duration and Mechanical Abrasion on Microplastic Fragmentation by Polymer Type*. Environmental Science & Technology, **2017**, 51(8): p. 4368-4376.

7. Hildebrandt, L., N. Voigt, T. Zimmermann, A. Reese, and D. Proefrock, *Evaluation of continuous flow centrifugation as an alternative technique to sample microplastic from water bodies*. Marine Environmental Research, **2019**, 151: p. 104768.

8. Domogalla-Urbansky, J., P.M. Anger, H. Ferling, F. Rager, A.C. Wiesheu, R. Niessner, N.P. Ivleva, and J. Schwaiger, *Raman microspectroscopic identification of microplastic particles in freshwater bivalves (Unio pictorum) exposed to sewage treatment plant effluents under different exposure scenarios*. Environ Sci Pollut Res Int, **2019**, 26(2): p. 2007-2012.

9. Lorenz, C., L. Roscher, M.S. Meyer, L. Hildebrandt, J. Prume, M.G.J. Löder, S. Primpke, and G. Gerdts, *Spatial distribution of microplastics in sediments and surface waters of the southern North Sea*. Environmental Pollution, **2019**, 252: p. 1719-1729.

10. Domogalla-Urbansky, J., P.M. Anger, H. Ferling, F. Rager, A.C. Wiesheu, R. Niessner, N.P. Ivleva, and J. Schwaiger, *Raman microspectroscopic identification of microplastic particles in freshwater bivalves (Unio pictorum) exposed to sewage treatment plant effluents under different exposure scenarios*. Environmental Science and Pollution Research, **2019**, 26(2): p. 2007-2012.

11. Cole, M., *A novel method for preparing microplastic fibers*. Scientific Reports, **2016**, 6(1): p. 34519.

12. Prata, J.C., J.L. Castro, J.P. da Costa, A.C. Duarte, T. Rocha-Santos, and M. Cerqueira, *The importance of contamination control in airborne fibers and microplastic sampling: Experiences from indoor and outdoor air sampling in Aveiro, Portugal*. Marine Pollution Bulletin, **2020**, 159: p. 111522.

13. Enders, K., R. Lenz, C.A. Stedmon, and T.G. Nielsen, *Abundance, size and polymer composition of marine microplastics ≥10µm in the Atlantic Ocean and their modelled vertical distribution*. Marine Pollution Bulletin, **2015**, 100(1): p. 70-81.

14. Kooi, M., J. Reisser, B. Slat, F.F. Ferrari, M.S. Schmid, S. Cunsolo, R. Brambini, K. Noble, L.-A. Sirks, T.E.W. Linders, R.I. Schoeneich-Argent, and A.A. Koelmans, *The effect of particle properties on the depth profile of buoyant plastics in the ocean*. Scientific Reports, **2016**, 6(1): p. 33882.

15. Brunner, K., T. Kukulka, G. Proskurowski, and K.L. Law, *Passive buoyant tracers in the ocean surface boundary layer: 2. Observations and simulations of microplastic marine debris*. Journal of Geophysical Research: Oceans, **2015**, 120(11): p. 7559-7573.

16. Lenaker, P.L., A.K. Baldwin, S.R. Corsi, S.A. Mason, P.C. Reneau, and J.W. Scott, *Vertical Distribution of Microplastics in the Water Column and Surficial Sediment from the Milwaukee River Basin to Lake Michigan*. Environmental Science & Technology, **2019**, 53(21): p. 12227-12237.

More Information

This application contains a share of ongoing work comprising method development and a large dataset, which are planned to be published in peer-reviewed scientific journal.

Agilent

Trusted Answers